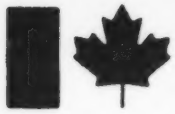

Environment Canada | Environnement Canada

National Water Research Institute | Institut National de Recherche sur les Eaux

Inland Waters Directorate | Direction Générale des Eaux Intérieures

Bishop (23)

Study H83 353

This manuscript has been submitted to

the Canadian Journal of [illegible]l Engineering

for publication and the contents are subject to change

FIELD ASSESSMENT OF FLOATING TIRE BREAKWATER

by

Craig T. Bishop

Shore Processes Section
Hydraulics Division
National Water Research Institute
Burlington, Ontario

September 1984

Field Assessment of Floating Tire Breakwater

Craig T. Bishop

Abstract

A field monitoring program of a Goodyear floating tire breakwater (FTB) was undertaken at La Salle Park, Burlington, Ontario during 1981 and 1982. Incident and transmitted waves were measured with underwater pressure transducers. The resulting wave height transmission data compares favourably with previous results from model studies. Mooring loads on some anchor lines were measured with two electronic and four mechanical gauges. The resulting peak load data, corresponding to incident wave heights up to 0.65 m, is in good agreement with previous results from prototype scale model studies.

KEYWORDS: coastal engineering, floating tire breakwaters, marinas, pressure gauges, mooring forces, waves

RÉSUMÉ

Un programme de contrôle sur le terrain d'une jetée flottante de pneus (JFP) a été entrepris au parc La Salle de Burlington (Ontario) en 81 et 82. Des vagues naissantes et transmises ont été mesurées au moyen de transducteurs de pression sous-marins. Les données de transmission de le hauteur des vagues qui en ont résulté se comparent avantageusement aux résultats obtenus auparavant dans des études menées sur des modèles. Les charges d'ammarage de certaines lignes de mouillage ont ête mesurées au moyen de deux jauges électroniques et de quatre jauges mécaniques. Les données sur les charges de pointe qui en ont résulté, correspondant à des hauteurs de vagues naissantes atteignant 0,65 m, sont en accord avec les résultats antérieurs provenant des études de prototypes.

MOTS-CLÉS: génie littoral, jetée flottante de pneus, ports de plaisance, baromètres, forces d'ammarage, vagues

MANAGEMENT PERSPECTIVE

Floating breakwaters made of automobile tires provide an efficient and effective way to utilize marine resources with little impact on the environment. This paper provides added proof to professional groups that the new breakwater is an acceptable solution for many places. The data and analysis lessen the uncertainties of performance and of the loading on anchors.

Floating tire breakwaters have a valid place in coastal engineering, especially where environmental factors must be respected.

T. Milne Dick
Chief, Hydraulics Division

PERSPECTIVE DE GESTION

Les jetées flottantes faites de pneus d'automobile fournissent un moyen efficace et utile d'utiliser des ressources marines sans trop porter atteinte à l'environnement. La présente étude fournit aux groupes professionnels une preuve additionnelle du fait que la nouvelle jetée constitue une solution acceptable à de nombreux endroits. Les données et leur analyse permettent de réduire les incertitudes du rendement et de la charge sur les ancres.

Les jetées flottantes de pneus jouent un rôle utile en génie littoral, particulièrement lorsqu'il faut protéger l'environnement.

T. Milne Dick
Chef
Division de l'hydraulique

Field Assessment of Floating Tire Breakwater

Craig T. Bishop

Hydraulics Division, National Water Research Institute, P.O. Box 5050

Burlington, Ontario, Canada L7R 4A6 (416) 637-4274

Introduction

Floating Tire Breakwaters (FTBs) originated in 1963 and are used mainly to provide wave protection at limited-fetch locations. Until recently, design information was only available from two-dimensional model tests. A large FTB of the Goodyear design, comprising 35,000 car tires, was constructed in Burlington, Ontario, in the spring of 1981. Its proximity to the National Water Research Institute provided an excellent opportunity to collect prototype performance data. Accordingly, a field monitoring program was initiated to measure wave transmission and mooring force characteristics. The resulting prototype design data is presented.

Site Description

La Salle Park is located on the north shore of Hamilton Harbour, at the western end of Lake Ontario. A location map, also showing bathymetry and fetches, is shown in Figure 1. The prevailing wind direction is from the southwest, especially during the May to October boating season. Strong winds also blow from the east and

northeast directions. The modest fetches at La Salle Park (less than 4.5 km) restrict typical significant wave heights and periods to less than 0.75 m and 3 s respectively, while extreme values are less than 1.25 m and 4 s respectively. Currents in the harbour near La Salle Park are negligible.

The moderate wave climate and relatively large water depths of 7 m or more make the FTB a practical wave protection alternative for the marina at this site. A conventional bottom-resting breakwater would be prohibitively expensive for a marina here. An FTB of the Goodyear design was assembled and installed in the Spring of 1981 (Figure 2).

The Goodyear design (Candle and Piper 1974) assembles basic modules, which consist of 18 tires in a 3-2-3-2-3-2-3 arrangement, into a flexible breakwater mat that is one layer of tires thick (Figure 3). The La Salle Park FTB uses conveyor belting to bind the tires together to form a module, and to interconnect the modules. The FTB mat is moored with steel chains to concrete gravity anchors. Construction details and costs for the La Salle Park FTB can be found in Bishop and Gallant (1981). State-of-the-art construction practices and materials are discussed in Bishop et al. (1983). Performance of the breakwater to date has been fully satisfactory. There have been no maintenance requirements during the first three years.

Design Information

A coastal engineer charged with designing an FTB has two main concerns requiring design data:

1. For a given incident wave height or wave energy spectrum, what will the transmitted wave height or wave energy spectrum be after propagating through the FTB?
2. For a given incident wave height or wave energy spectrum, how big will the mooring loads be?

Other concerns include the effect of ice on the FTB and its mooring system, the drag force on the FTB due to currents (Bishop 1981), and continued flotation of the breakwater (Bishop 1982).

An earlier Goodyear FTB field monitoring program was undertaken in Narragansett Bay, Rhode Island (Kowalski and Candle 1976) but no useful design information was ever published. The Goodyear FTB design information that does exist is the result of model tests conducted in wave flumes, some at prototype scale.

Instrumentation

Waves were measured with four pressure transducers (Viatran Corporation, Model 218), two on each side of the 64 x 9 module (129 m x 19 m) FTB test section (Figure 4). The pressure transducers were

mounted on vertical steel pipes (8 cm diameters) that had been driven into the harbour bottom. The depth of submergence of the transducers was approximately 1.06 m below International Great Lakes Datum (IGLD). The depth of water at the seaward transducer locations was 7.2 m below IGLD, and 6.6 m below IGLD at the leeward locations. During the course of the study, the mean water level varied from 35 to 70 cm above IGLD.

The pressure transducers were calibrated in a static test in the NWRI Calibration Lab. Changes between pre- and post-season calibrations were less than one percent.

It was intended to measure the mean incident wave direction using the two seaward transducers as done by Bruno et al. (1980). However, the separation between the two transducers as installed in the field was 6.4 m, and this was much larger than the specified separation of 3.5 m. Accordingly, the directional results suffered from spatial aliasing and were not used.

Mooring loads were measured with two electronic load cells (manufactured by Sensotec Inc.) and four mechanical "scratch" gauges. The centre mooring line on the seaward side was equipped with a 4000 lb (17800 N) electronic load cell, mounted on the chain mooring line about 2 m below the mean water level. The northwest corner mooring line was equipped with a 2500 lb (11100 N) electronic load cell, mounted about 2 m below mean water level. The water depths at the two locations were approximately 6.7 and 3.1 m below IGLD respectively. The ratio of the length of mooring line to the water depth was measured to be approximately 4, except at the northwest corner where it was 5.4. A third

electronic load cell for the southwest corner mooring line was installed but did not work.

Wind velocity data was obtained from a cup anemometer and vane installed on a tower on La Salle Park Wharf (Figure 4) at an elevation of 10 m above mean water. The anemometer was calibrated in NWRI's towing tank for speeds up to 6 m/s. The difference between pre- and post-season calibrations was -2.6 percent. The post-season value was used. The compass was calibrated on the tower with readings taken by pointing the vane at known reference locations around the harbour. Bearings were then determined accurately from a map.

The pressure, load and wind sensors were connected to a 12-channel Sea Data logger via a custom built control unit (Valdmanis and Savile 1984). The control unit activated the logger whenever the wind speed and direction met pre-set conditions. This limited recording observations to significant events. A nine-minute sample of data would be collected at 2 Hz, followed by a 51-minute gap. At the beginning of the next hour, the control unit would check the wind conditions to determine whether to start collecting another sample.

In order to improve the resolution of the data gathering system, a duplicate set of the pressure signals with the means removed was amplified 21.8 times and stored along with the other data on cassettes by the Sea Data logger (Valdmanis and Savile 1984).

Wave Pressure to Wave Height Transfer Function

According to linear theory for gravity waves, a subsurface wave pressure head fluctuation H_p, can be related to the surface wave height, H, by

$$[1] \qquad H = H_p \frac{\cosh kh}{\cosh k(h+z)}$$

where k is the wave number $2\pi/L$, L is the wavelength in water depth, h, and z is the depth of submergence of the pressure transducer, measured upward from the still water level. The term $(\cosh k(h+z)/\cosh kh)$ is known as the pressure response factor, K_p.

An empirical correction factor, N, has been introduced to Equation 1 by many investigators:

$$[2] \qquad H = N \cdot H_p \frac{\cosh kh}{\cosh k(h+z)}$$

A relation for N was determined from prototype scale tests conducted in the 103 m long wind-wave flume of the National Water Research Institute. These tests are reported elsewhere (Bishop 1984). Several empirical relations for N versus $|z|/L$ are shown in Figure 5.

The measured pressure head fluctuations were analyzed using fast Fourier transform techniques. Then the power spectral components, $S_s(f)$, of the water surface elevation were related to the power spectral components of the subsurface pressure head variation, $S_p(f)$, by

[3] $$S_s(f) = \left(\frac{N(f)}{K_p(f)}\right)^2 \cdot S_p(f)$$

using values for N(f) from Bishop (1984).

Wave Transmission

Mooring load and amplified pressure signals for the largest recorded event are shown in Figure 6. Dimensional analysis (Harms et al. 1981) has shown that the transmission coefficient C_t, where C_t is the ratio of transmitted to incident wave heights (H_t/H_i), can be expressed as

[4] $$C_t = \psi(L/B, H/L, D_t/h, B/D_t)$$

For the La Salle Park FTB, $B/D_t = 29.5$ and $D_t/h = 0.085$ at the pressure transducer locations. Model tests of Goodyear FTB's (Harms and Bender 1978) showed that wave transmission is insensitive to the B/D_t parameter or the D_t/h parameter for $D_t/h \leq 0.32$. Values of H_c/L_p were typically 0.04 to 0.08.

Wave transmission results are given in terms of transmission coefficients, $C_t(f)$, versus the ratio of wavelength, L(f), to breakwater beam, B, where

[5] $$C_t(f) = \left[\frac{S_{st}(f)}{S_{si}(f)}\right]^{1/2}$$

and $S_{st}(f)$ is the average of the two leeward gauges (transmitted waves) and $S_{si}(f)$ is the average of the two seaward gauges (incident waves). It should be noted that values of C_t for any given frequency are independent of the correction factor N(f). Figure 7 shows transmission results for $S_i(f)/S_i(f_p) > 0.10$ and $f_p < 0.67$ Hz and the corresponding second order regression curve. There is good data coverage for $0.2 \leq L/B \leq 0.8$. This range has been extended in Figure 8 by plotting results for the two values of frequency (at 0.04 Hz intervals) for each record that are just smaller than the smallest frequency meeting the criterion $S_i(f)/S_i(f_p) > 0.10$. The corresponding second order regression curve is also shown. This provides good data coverage for $0.8 \leq L/B \leq 1.4$.

The data plotted in Figures 7 and 8 is from 118 records obtained between October 8 and November 13, 1982. Characteristic wave heights vary from 12 to 66 cm with peak frequencies from 0.32 Hz to 0.64 Hz.

The data in Figures 7 and 8 has been combined in Figure 9. The curve through the data is the curve from Figure 7 for $0.2 \leq L/B \leq 0.6$, from Figure 8 for $1.0 \leq L/B \leq 2.2$, and a transition by eye for $0.6 \leq L/B \leq 1.0$.

Some of the scatter in results is probably due to variability in the direction of the incident waves. Under oblique attack, the effective beam of the FTB is increased but this has not been taken into account. A constant value of B = 18.9 m was used to determine values of L/B.

Comparison With Model Results

Prototype scale wave transmission tests of Goodyear FTB's were conducted by Giles and Sorensen (1978) with car tires of 64 cm diameter using monoperiodic waves with heights up to 1.4 m. The tests were done on two different beam widths, four and six modules at two water depths, 2 and 4 m. Their results are referred to as the CERC results in Figure 10.

Model scale tests of Goodyear FTB's were conducted by Nelson (1978) using monoperiodic waves and tires of 15 cm diameter. The tests were done on three different beam widths, three, four and six modules at two water depths, 46 and 84 cm. Results for the six-module beam tests agree well with the CERC six-module results and these data sets have been plotted in Figure 11. Only those points with wave steepnesses H/L in the range 0.02 - 0.06 are included. The results are easily distinguishable because the CERC data is for $L/B \geq 0.81$ and the Nelson data is for $L/B \leq 0.82$. The curve through the data is from second order regression, modified slightly by eye for $L/B > 2.0$.

Model scale tests of Goodyear FTB's were conducted by Harms and Bender (1978) using mostly monoperiodic waves and tires of 8.4 and 15 cm diameter. The tests were done on four different beam widths, two, four, eight and twelve modules at water depths from 31 to 120 cm. Their results are referred to as the Harms results in Figure 10.

Model scale tests of Goodyear FTB's were conducted by McGregor (1978) using pseudo-random waves and tires of 15 cm diameter. The tests

were done on six different beam widths, 2, 3, 4, 5, 6 and 7 modules at a constant water depth of 240 cm. Results were presented graphically in the form of transmission coefficients versus frequency for each beam width (McGregor 1978, Figure 7). All tests were run with the same incident wave spectrum with a peak frequency of 0.67 Hz. Values of C_t versus L_p/B have been obtained by measurement from McGregor's Figure 7. Results agree very well with those of Harms and are shown in Figure 10. Unfortunately, there is no data for $L_p/B < 0.99$.

As seen in Figure 10, the results of the present field study agree quite closely with earlier model test results. For practical purposes, the most important part of Figure 10 is for values of C_t less than 0.5. In this range the Harms curve shows the best agreement with the field results. For values of C_t larger than 0.4, the Harms and McGregor results underpredict C_t.

The field results indicate a levelling-off or residual value of C_t of approximately 0.15 while the model results tend towards zero for small values of L/B. This may be attributable to viscous scale effects causing more attenuation in the model than in prototype. It may also be due to reflected and diffracted wave energy contributions in the field. Unfortunately the prototype scale CERC model tests do not include data for values of L/B less than 0.8.

Application

Wave energy spectra for the largest recorded wave height event are shown in Figure 12. For a known incident spectrum the transmitted spectrum can be predicted using values of C_t from Figure 10. Using the La Salle Park curve, this has been done for pressure transducers 3 and 5 in Figure 4; results are provided in Table 1. The predicted transmitted characteristic wave height is 0.193 m while the value calculated from the pressure measurements is 0.184 m, giving an overprediction of 4.9 percent.

A simpler approach to predicting the transmitted wave height would be to use a single value of C_t corresponding to the peak frequency. For the example in Table 1, f_p = 0.36 Hz giving C_t = 0.355. The predicted transmitted wave height would be 0.638 x 0.355 = 0.226 m, giving an overprediction of 25 percent. In general, the simpler approach will be less accurate than the spectral approach. Whenever the incident spectrum is multi-peaked, only the spectral prediction method should be used.

For practical purposes, a breakwater is seldom required unless wave attenuation of 50 percent or more is needed. From Figure 10 it can be seen that to obtain $C_t < 0.5$ the ratio L/B must be less than 0.85. Therefore, a rule of thumb for Goodyear FTB's would be that the beam must be at least 1.2 times the design wavelength. For another type of FTB, the Pipe-Tire floating breakwater (Harms et al. 1981), a comparable

rule of thumb would be that the beam must be at least 0.8 times the design wavelength.

Mooring Loads - Empirical

Mooring load signals from the largest recorded wave height event are shown in Figure 6. It can be seen that the mooring load fluctuates with the passage of each wave. There is a well-defined minimum load on each gauge during a record, and local maxima which appear to be correlated with wave groups.

Dimensional analysis of wave-induced mooring loads (Harms et al. 1981) has shown that

$$[6] \qquad F_d = \phi(L/D_t,\ H/D_t,\ D_t/h,\ B/D_t)$$

where F_d is the dimensionless peak mooring load, D_t is the outside tire diameter (approximately 64 cm) and

$$[7] \qquad F_d = \frac{F_{max}\cos\theta}{\ell\ \rho g D_t^{\,2}}$$

where F_{max} is the maximum measured load (Newtons) at a gauge during a record

ρ density of fresh water in kg/m^3

g gravitational acceleration (m/sec^2)

ℓ is the length in metres of breakwater frontage restrained by the mooring line (10.72 m for the central line, 5.36 m for the corner line).

θ is the angle between the mooring line and a perpendicular to the front face of the FTB. (0 degrees for the central line, 45 degrees for the corner line)

The formulation of Equation 6 neglects current or ice-induced mooring loads; it is appropriate for the La Salle Park FTB during the boating season.

Model tests of Goodyear FTB's (Harms and Bender 1978) and of Pipe-Tire floating breakwaters (Harms et al. 1981) revealed that F_d does not vary substantially with B/D_t. Mooring loads increase with increasing values of L/D_t, H/D_t and D_t/h.

Preliminary analysis of the dimensionless parameters F_d versus H_c/D_t showed that the use of tires with diameters larger than 0.64 m would result in the prediction of smaller mooring loads for the same incident wave height. This disagrees with expectations. More data is needed to quantify the effect of tire diameter on mooring loads. Accordingly, the analysis of mooring loads has been done dimensionally.

The dominant variable affecting mooring loads at the La Salle Park FTB is H_c. There are 65 records in which $H_c \geq 30$ cm (see Tables 2-4). For these records, the dimensional peak mooring loads per unit length $(F_{max}\cos\theta)/\ell$ have been plotted against H_c in Figure 13.

After removing several outlying points from the data set, second order regression curves were determined and are also shown in Figure 13*. Some of the scatter in results is probably due to L_p varying from 5.75 m to 15.2 m. However, there is insufficient data at overlapping values of H_c to determine a relation similar to that between F_d and L_p/D_t as done for Pipe-Tire floating breakwaters in Harms et al. (1981).

Results from the 6-module-beam two-dimensional prototype scale tests by Giles and Sorensen (1978) in 4 m of water are compared with the La Salle Park results in Figure 14. For the Giles and Sorensen (1978) data, the height H of regular waves has been substituted for H_c. Agreement is surprisingly good. A second order regression analysis of the 64 field test points and 39 model test points gives

$$[8] \qquad (F_{max}\cos\theta)/\ell = -346 + 8.76\, H_c + 0.0798\, (H_c)^2$$

where $(F_{max}\cos\theta)/\ell$ is in Newtons per metre length and H_c is in centimetres. The corresponding value of the square of the correlation coefficient is 0.96. Equation 8 should only be used for values of $H_c > 40$ cm. It is very similar to the relation proposed by Harms and

---

* A plot of $(F_{max}\cos\theta)/\ell$ versus H_c where H_c was calculated according to linear wave theory (i.e., N = 1.0) showed almost no difference in the regression curve over the range of data.

Westerink (1980) from an analysis of the 6-module-beam data of Giles and Sorensen (1978) in 4 m of water which gave $F_{max}/\ell = .140\ (H_c)^2$.

A striking feature of Figure 13 is that the mooring loads on the corner line ($D_t/h = 0.18$) are significantly greater than those at the central line ($D_t/h = 0.085$). Prototype scale model tests of Pipe-Tire floating breakwaters (Harms and Westerink 1980) showed a large increase in mooring loads when D_t/h changed from 0.22 to 0.51. Prototype scale model tests of Goodyear FTB's (Giles and Sorensen 1978) showed a slight decrease in mooring loads when D_t/h changed from 0.16 to 0.32. This latter trend, however, disagrees with the results of other model studies (Harms 1979) and with theoretical expectations. At La Salle Park, the increase in D_t/h from 0.085 to 0.18 is not expected to cause a large increase in mooring loads. A more likely reason for the increase in mooring loads from central to corner mooring lines is that waves diffract around the corner of the breakwater, essentially doubling the frontage restrained by the corner line. Clearly more data is needed on the influence of relative draft D_t/h on mooring forces. Meanwhile, for design purposes, it is suggested that the mooring load (in a direction perpendicular to the FTB length) of the corner line be estimated as twice the central mooring line load.

Mooring Loads - Analytical

The preceding empirical approach can be compared with an analytical method. A floating body which reflects or dissipates wave

energy is subject to a mean horizontal force, F. The existence of a horizontal momentum flux, or radiation stress, has been demonstrated experimentally by Longuet-Higgins (1977). For non-breaking waves of low amplitude (obeying linear wave theory), the mean horizontal force per unit length has been shown by Longuet-Higgins (1977) by conservation of momentum to be

$$[9] \qquad F = \frac{\rho g}{4}\left(a_i^2 + a_r^2 - a_t^2\right)\left(1 + \frac{2kh}{\sinh 2kh}\right)$$

where ρ = density of water

g = gravitational acceleration

a_i = the amplitude of the incident wave

a_r = the amplitude of the reflected wave

a_t = the amplitude of the transmitted wave

$k = 2\pi/L$

L = wavelength

h = water depth

Floating tire breakwaters characteristically dissipate wave energy through internal friction rather than reflection. Therefore, as a first approximation, F has been calculated by assuming $a_r = 0$. The wave amplitude is assumed to be half the wave height. For the water depths and wavelengths present at La Salle Park, the factor $(1 + 2kh/\sinh kh)$ equals unity. In Figure 15, the predicted loads (for a 5-module

frontage of 10.72 m) are compared to the peak loads measured at the central mooring line. Equation (9) tends to overpredict for loads less than 2000 N and to underpredict for larger loads. It should not be used for design purposes, contrary to some evidence presented in Galvin and Giles (1979) which gave $F = F_{max}/2$. This lack of agreement can be attributed to the following reasons:

- The theory predicts a mean load in non-breaking waves but steep and breaking waves were present at La Salle Park. Furthermore, the comparison of mean loads estimated by Equation (9) is made with the peak measured loads (a comparison of F to $F_{max}/2$ is also unsatisfactory).
- The theory is valid for sinusoidal waves. In irregular waves, the wave amplitude has been approximated by one-half the characteristic wave height.
- The peak prototype mooring loads are dependent on the elasticity of the mooring lines and on the dynamic interaction between the waves and the structure. Wave grouping and the structure's natural period of oscillation will affect the peak mooring loads, while the mean horizontal load is essentially independent of wave-structure dynamics and mooring line elasticity.

Mechanical Load Gauge

A mechanical load gauge was installed on each of four windward anchor chains (Figure 4). The load gauges produce scratches on brass disks that rotate as the scratch is being made. After retrieving the disks at the end of the field season the scratches were measured using a microscope. This provided estimates of the largest loads but did not give the load-time history. The gauges were designed for a maximum load of 5000 lbs (22250 N). They were calibrated in the lab and showed a linear relationship between the load and the length of the scratch up to 22250 N.

The gauges were deployed September 24 - November 12, 1981 and June 15 - November 15, 1982. The largest measured loads were much smaller than the design load of 22250 N, and therefore, the resolution of the scratches was sometimes difficult. The maximum estimated loads (N ± 20 percent) for gauges 1 to 4 for 1981 and 1982 respectively were:

	1	2	3	4
1981	4900	3400	3700	3900
1982	-	5900	4400	5400

These estimates compare well with the maximum loads measured in 1982 with the electronic load cells: 5400 N at the central anchor chain between gauges 2 and 3, and 6300 N at the corner anchor chain beside gauge 4. These loads were probably induced by characteristic wave heights of 65 cm or less.

Storm of April 30, 1984

A severe storm occurred over the Great Lakes on this date. A fishing boat sank near the end of Long Point in Lake Erie, taking three lives. Several sailboats moored at offshore buoys beside the La Salle Park Marina broke their mooring lines and sunk or were badly damaged. One of these breakaways became grounded on the 9-module wide southwest-facing section of FTB; the boat safely rode out the storm without damage to itself or the FTB.

Although the FTB was not equipped with measuring instrumentation during this storm, its performance was observed under these extreme wave conditions. Environment Canada wind measurements at Hamilton Airport, located 14 km south of La Salle Park, recorded a peak southwest gust of 30.9 m/s at 1555 hours, with a corresponding one-minute average speed of 21.6 m/s. At the L.B. Pearson (Toronto) International Airport, the peak of the storm occurred at 1422 hours with a southwest gust of 27.8 m/s and a one-minute average speed of 19.6 m/s. Using the average of these two one-minute speeds, 20.6 m/s, the resulting hindcast wave conditions at La Salle Park are H_c = 1.0 m and T_p = 3.5 s.

The FTB successfully rode out the storm without any apparent damage. Minor damage occurred to the floating docks in two locations. The FTB mooring system had been designed for waves of the magnitude and period hindcast for this storm. However, the transmitted characteristic wave heights were not expected to meet the standard of being less than 0.3 m.

The transmitted wave height at the peak of the storm has been estimated by obtaining a value of C_t from Figure 10 for L/B corresponding to T_p = 3.5 s; the resulting value of H_t is 0.66 m. Visual estimates of the transmitted wave height at the peak of the storm were 0.6 - 0.9 m.

An estimate of the peak mooring load can be obtained by using Equation 8 for H_c = 1.0; the resulting peak mooring load on a central mooring line is 14240 N or 1330 N/m.

Conclusions

The Goodyear-design floating tire breakwater at La Salle Park Marina has performed successfully from its installation in May 1981. It survived extreme wave conditions estimated at H_c = 1.0 m and T_p = 3.5 s with no damage, during a storm on April 30, 1984. It appears that an FTB of this type can be designed with confidence using the prototype results in this report and field-proven construction guidelines reported elsewhere (Bishop et al. 1983).

An 129 m x 19 m section of FTB was monitored during parts of 1981 and 1982. Wave transmission characteristics were determined by measuring incident and transmitted waves with underwater pressure transducers. The wave transmission results (Figure 10) are in close agreement with earlier results from model tests.

Mooring load characteristics were determined by measuring the loads exerted on several anchor lines using electronical and mechanical

gauges. For the central anchor line the peak mooring loads per unit length were found to be in good agreement with those measured in earlier prototype scale model tests (Figure 14). The peak loads measured on the corner anchor line were found to be significantly greater than those measured at the central anchor line.

Acknowledgements

Thanks are expressed to the City of Burlington for cooperation in the monitoring program, to Messrs. J. Valdmanis and M. Pedrosa for their help with the electronic system, to Mr. H. Savile for his work on the mechanical load gauges and in the field, and to Drs. T.M. Dick and M.G. Skafel for their continued support of this project over three years.

References

Bishop, C.T. 1981. Drag Tests on Pipe-Tire Floating Breakwater. National Water Research Institute, Burlington, Ontario.

Bishop, C.T. 1982. Floating Tire Breakwater Buoyancy Requirements. National Water Research Institute, Burlington, Ontario.

Bishop, C.T. 1984. Measuring Waves with Pressure Transducers. National Water Research Institute, Burlington, Ontario.

Bishop, C.T. and Gallant, B.A. 1981. Construction of Goodyear Floating Tire Breakwater at La Salle Marina, Burlington, Ontario. Proceedings of the 2nd Floating Breakwaters Conference, Dept. of Ocean Engineering, University of Washington, Seattle, Washington, 190-207.

Bishop, C.T. DeYoung, B., Harms, V.W. and Ross, N.W. 1983. Guidelines for the Effective Use of Floating Tire Breakwaters. Information Bulletin 197, Cornell University Cooperative Extension, Ithaca, New York.

Bruno, R.O., Dean, R.G. and Gable, C.B. 1980. Longshore Transport Evaluation at a Detached Breakwater. Proceedings 17th Coastal Engineering Conference, American Society of Civil Engineers, 2:1453-1475.

Candle, R.D. and Piper, D.R. 1974. The Proposed Goodyear Modular Mat Type Scrap Tire Floating Breakwater. Goodyear Tire and Rubber Co., Akron, Ohio.

Draper, L. 1957. Attenuation of Sea Waves with Depth. La Houille Blanche, Vol. 12, 6:926-931.

Galvin, C. and Giles, M. 1979. Mooring Forces on Rafts from In-Line Radiation Stress. Proceedings Civil Engineering in the Oceans, American Society of Civil Engineers, 487-503.

Giles, M.L. and Sorensen, R.M. 1978. Prototype Scale Mooring Load and Transmission Tests for a Floating Tire Breakwater. Technical Paper 78-3. U.S. Army Corps of Engineers, Coastal Engineering Research Center, Fort Belvoir, Virginia.

Grace, R.A. 1978. Surface Wave Heights from Pressure Records. Coastal Engineering, 2:55-67.

Harms, V.W. 1979. Design Criteria for Floating Tire Breakwaters. Journal of the Waterway, Port, Coastal and Ocean Division, ASCE, WW2:149-170.

Harms, V.W. and Bender, T.J. 1978. Preliminary Report on the Application of Floating Tire Breakwater Design Data. Water Resources and Environmental Engineering Research Report 78-1, Dept. of Civil Engineering, State University of New York at Buffalo.

Harms, V.W. and Westerink, J.J. 1980. Wave Transmission and Mooring Force Characteristics of Pipe-Tire Floating Breakwaters. Report LBL-11778, University of California, Berkeley, California.

Harms, V.W., Bishop, C.T. and Westerink, J.W. 1981. Pipe-Tire Floating Breakwater Design Criteria. Proceedings of the 2nd Floating Breakwaters Conference, Dept. of Ocean Engineering, University of Washington, Seattle, Washington, 47-86.

Kowalski, T. and Candle, R.D. 1976. Scrap Tire Floating Breakwater. Proceedings Oceans '76, 886-894.

Longuet-Higgins, M.S. 1977. The Mean Forces Exerted by Waves on Floating or Submerged Bodies with Applications to Sand Bars and Wave Power Machines. Proceedings Royal Society of London, A352:463-480.

McGregor, R.C. 1978. The Design of Scrap-Tyre Floating Breakwaters with Special Reference to Fish Farms. Proceedings Royal Society of Edinburgh, 76B:115-133.

Nelson, W.L. 1978. An Investigation into the Scaling Confidence of Floating Tire Breakwater Model Tests. A thesis submitted in partial fulfillment of the requirements for the degree of Master of Science in Engineering, University of Washington, Seattle, Washington, 79 p.

Shooter, J.A. and Ellis, G.E. 1967. Surface Waves and Dynamic Bottom Pressure at Buzzard's Bay, Massachusetts. Defence Research Laboratory Accoustical Report 292, University of Texas, Austin, Texas.

Valdmanis, J. and Savile, H.A. 1984. Hardware for 1982 Monitoring of Floating Tire Breakwater at La Salle Park Marina. National Water Research Institute, Burlington, Ontario.

LIST OF SYMBOLS

a_i	amplitude of the incident wave
a_r	amplitude of the reflected wave
a_t	amplitude of the transmitted wave
B	beam width of FTB
C_t	transmission coefficient = H_t/H_i
D_t	tire diameter
f_p	frequency corresponding to the peak of the wave energy spectrum
f	frequency
FTB	floating tire breakwater
F	mean horizontal force per unit length
F_d	dimensionless peak mooring load
F_{max}	maximum measured load during a record
g	gravitational acceleration
h	water depth
H	wave height
H_c	characteristic wave height = four times the standard deviation of the water surface elevation record
H_i	incident wave height
H_p	wave pressure head
H_t	transmitted wave height
IGLD	International Great Lakes Datum
k	$2\pi/L$
K_p	pressure response factor
L	wavelength

List of Symbols (continued)

L_p	wavelength corresponding to the frequency at the peak of the wave energy spectrum
ℓ	length of breakwater frontage
N	empirical correction factor for pressure records
$S_i(f)$	water surface variance spectral component of incident waves
$S_t(f)$	water surface variance spectral component of transmitted waves
$S_s(f)$	water surface variance spectral component
$S_p(f)$	wave pressure head variance spectral component
T_p	wave period = $1/f_p$
z	depth of submergence of pressure transducer

Greek

ρ	density of fresh water
θ	angle between the mooring line and a perpendicular to the front face of the FTB

TABLE 1. Comparison of Transmitted Wave Energy Spectral Values

(1982/11/12, 1117 hours)

(1) freq (Hz)	(2) $\frac{L}{B}$	(3) $S_i(f)$ (cm^2/Hz)	(4) $S_t(f)$ (cm^2/Hz)	(5) C_t	(6) $C_t^2 \cdot S_i(f)$ (cm^2/Hz)
.24	1.43	3.5	2.3	.795	2.2
.28	1.05	46.3	24.4	.675	21.1
.32	.81	424.6	83.9	.515	112.6
.36	.64	2054.8	273.2	.355	259.0
.40	.52	1581.1	78.0	.260	106.9
.44	.43	870.5	23.5	.215	40.2
.48	.36	457.0	11.2	.185	15.6
.52	.31	242.0	8.2	.175	7.4
.56	.26	256.1	5.5	.165	7.0
.60	.23	122.9	4.6	.155	2.7
.64	.20	163.4	4.2	.150	3.7
.68	.18	143.7	7.5	.150	3.2
	H_c(m):	.638	.184		.193

(4) Spectral values calculated from measured pressure fluctuations on leeward side.

(5) From Figure 10

(6) Predicted spectral values from (3) and (5)

(7) The values of H_c differ slightly from those in Table 4 due to a simplified manual method of computation here.

TABLE 2. Summary Data Table for Mooring Force Results When $H_c \geq 30$ cm

Date	Time (hr/min)	T_p (s)	L_p (m)	H_c (cm)	F_{max}/ℓ central line (N/m)	$F_{max}\cos 45°/\ell$ corner line (N/m)
Oct. 20	7/7	1.92	5.75	36.4	52.6	(72.5)*
	9/8	2.08	6.77	39.1	64.8	(85.4)
	10/8	2.27	8.06	54.3	166.0	(223.2)
	11/7	2.50	9.75	50.0	225.2	255.6
	12/7	2.27	8.06	49.2	152.3	389.1
	13/8	2.08	6.77	33.8	75.3	98.4
	14/8	2.08	6.77	36.9	113.4	201.7
	15/8	2.27	8.06	44.1	161.2	367.7
	16/8	2.78	12.0	48.6	159.6	374.8
	17/8	2.78	12.0	49.0	192.8	435.9
	18/8	2.08	6.77	37.5	93.2	207.5
	19/8	2.50	9.75	40.0	106.1	316.7
	20/8	2.50	9.75	42.1	123.1	285.7
	21/8	2.27	8.06	39.9	116.7	322.4
	22/8	2.50	9.75	45.1	140.9	356.8
	23/8	2.50	9.75	46.2	123.9	380.6
Oct. 21	0/8	2.27	8.06	30.8	(277.0)	213.9
	1/8	2.50	9.75	36.1	108.5	295.1
	2/8	2.50	9.75	38.4	69.6	193.9
	3/8	2.50	9.75	34.4	72.1	196.7
	4/8	2.27	8.06	35.1	82.6	201.7
	5/7	2.27	8.06	30.2	51.8	121.4

* Brackets signify an outlying point

TABLE 3. Summary Data Table for Mooring Force Results When $H_c \geq 30$ cm

Date	Time (hr/min)	T_p (s)	L (m)	H_p (cm)	F_{max}/ℓ central line (N/m)	$F_{max}\cos 45°/\ell$ corner line (N/m)
Nov. 5	11/30	2.50	9.75	37.3	79.3	129.9
	12/30	2.27	8.06	32.3	64.0	133.6
	14/30	2.50	9.75	33.8	57.5	150.1
	15/31	2.50	9.75	41.9	85.8	257.0
	16/31	2.27	8.06	33.0	61.6	137.2
	18/31	2.27	8.06	33.0	72.1	162.9
	19/31	2.08	6.77	31.5	60.8	155.8
	20/31	2.27	8.06	36.5	70.5	139.3
	21/31	2.50	9.75	37.3	93.2	207.5
	23/31	2.50	9.75	37.3	85.8	213.3
Nov. 6	0/31	2.08	6.77	37.6	74.5	183.8
	1/31	2.27	8.06	38.7	72.1	219.0
	2/31	2.27	8.06	45.1	90.7	213.9
	3/31	2.50	9.75	44.5	99.7	321.7
	4/31	2.27	8.06	35.5	77.0	150.8
	5/31	2.08	6.77	35.3	69.6	135.8
	6/31	1.92	5.75	31.7	44.6	99.8
	7/31	2.08	6.77	32.1	52.6	105.6
	8/31	2.08	6.77	34.9	72.1	133.6
	9/31	2.08	6.77	36.0	68.8	139.3
	10/30	2.27	8.06	32.4	68.8	173.8
	11/33	2.08	6.77	31.2	53.4	109.9
	12/33	2.27	8.06	36.2	72.9	178.7
	13/33	2.27	8.06	38.1	69.6	147.1
	14/33	1.92	5.75	33.6	60.8	117.8
	15/33	2.27	8.06	41.2	73.7	218.3

TABLE 4. Summary Data Table for Mooring Force Results When $H_c \geq 30$ cm

Date	Time (hr/min)	T_p (s)	L (m)	H_p (cm)	F_{max}/ℓ_c central line (N/m)	$F_{max}\cos 45°/\ell_c$ corner line (N/m)
Nov. 12	0/11	1.92	5.75	30.2	47.8	(268.5)*
	2/13	1.92	5.75	32.3	60.8	114.1
	7/17	2.08	6.77	42.4	195.2	220.4
	8/17	2.27	8.06	46.4	237.3	336.7
	9/17	2.50	9.75	57.5	290.0	503.3
	10/17	2.50	9.75	55.2	321.6	812.1
	11/17	2.78	12.0	65.4	504.6	835.1
	12/17	2.27	8.06	44.7	214.7	355.4
	13/17	2.50	9.75	42.4	222.7	479.6
	14/17	2.08	6.77	41.1	179.0	(601.7)
	16/17	2.78	12.0	54.1	353.1	657.0
	17/17	2.78	12.0	59.8	406.6	545.4
	18/17	2.78	12.0	42.4	131.2	414.3
	19/17	3.13	15.2	35.3	81.0	188.8
	20/17	2.50	9.75	43.9	154.7	319.5
	21/17	2.27	8.06	30.7	46.9	108.5
	22/19	2.27	8.06	30.2	42.1	99.1

* Brackets signify an outlying point

FIGURE CAPTIONS

1. Location of La Salle Park.
2. Aerial view of FTB at La Salle Park Marina.
3. Detailed arrangement of tires in a Goodyear FTB.
4. Layout of instrumentation for La Salle Park field monitoring study.
5. Empirical relations for correction factor N for transfer function from wave pressure to wave height.
6. Mooring load and amplified pressure signals for the largest recorded event (82/11/12, 1117 hours).
7. Wave transmission results for $S_i(f)/S_i(f_p) \geq 0.10$ and $f_p < 0.67$ Hz.
8. Wave transmission results for $S_i(f)/S_i(f_p) < 0.10$ and $f_p < 0.67$ Hz.
9. Wave transmission results from 118 records obtained between October 8 and November 12, 1982, at La Salle Park.
10. Comparison of wave transmission curves.
11. Wave transmission results of Nelson (1978) and Giles and Sorensen (1978).
12. Wave energy spectra for the largest recorded event (82/11/12, 1117 hours).
13. Dimensional plot of peak mooring load versus characteristic wave height data.
14. La Salle Park peak mooring load data from central mooring line and 6-module-beam data from Giles and Sorensen (1978).
15. Comparison of measured peak mooring loads to predictions using relation of Longuet-Higgins (1977).

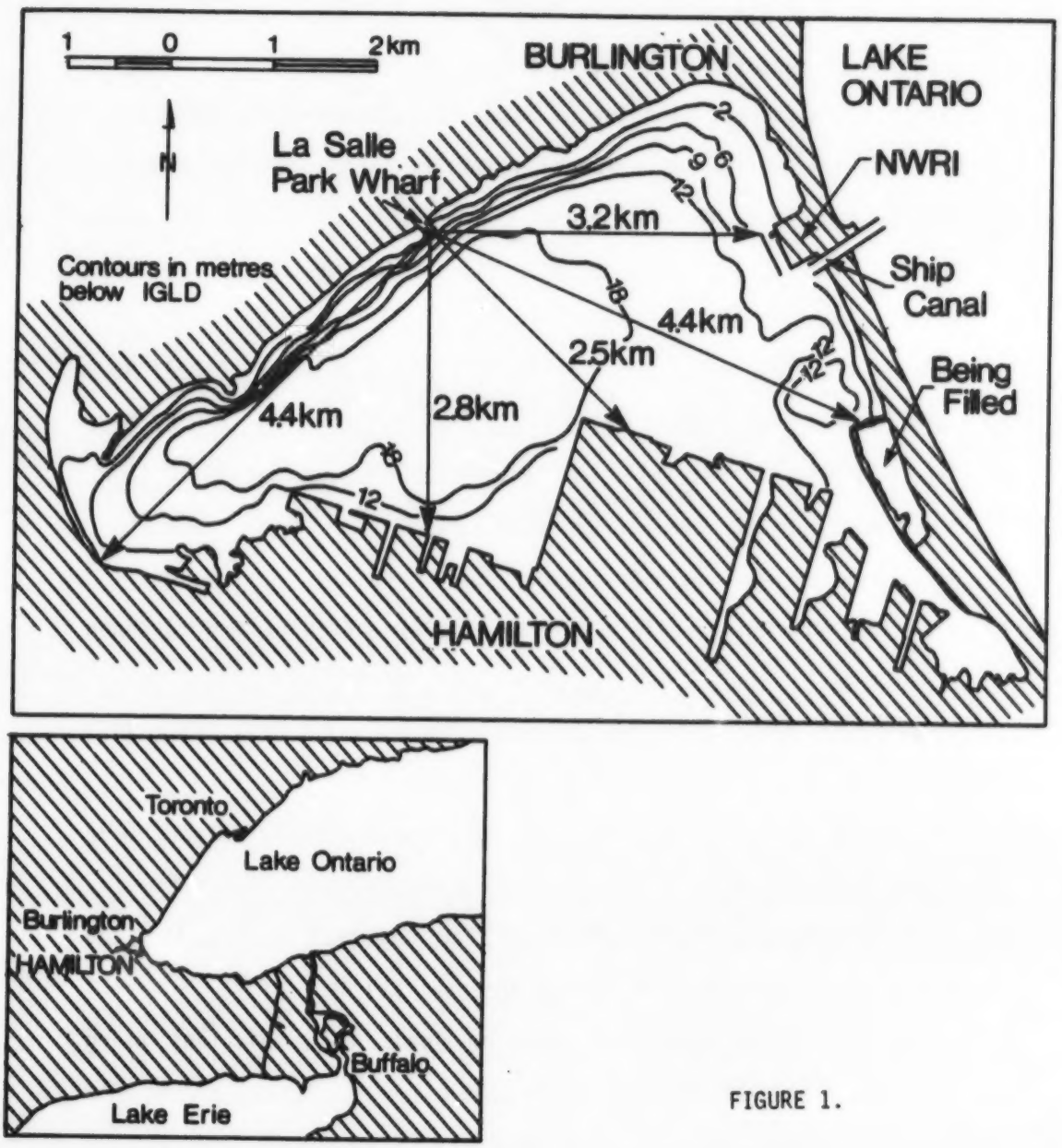
1 0 1 2km
N
BURLINGTON
LAKE ONTARIO
La Salle Park Wharf
NWRI
Contours in metres below IGLD
3.2km
Ship Canal
4.4km
2.5km
Being Filled
4.4km
2.8km
HAMILTON

Toronto
Lake Ontario
Burlington
HAMILTON
Buffalo
Lake Erie

FIGURE 1.

FIGURE 2.

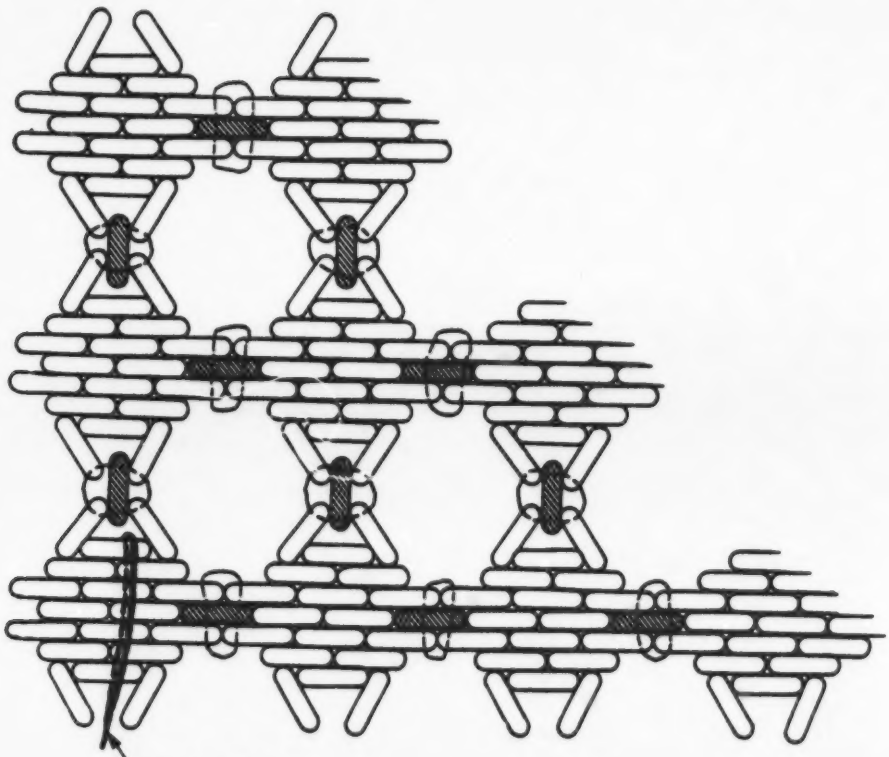

PLAN

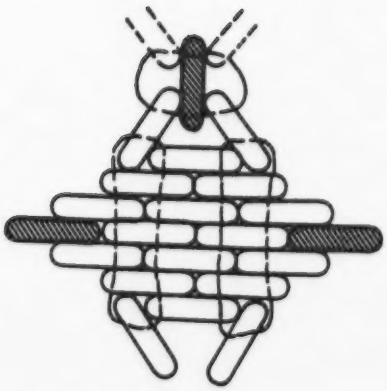

18 Tire Module Detail

Note: each tire equipped with some form of supplemental flotation, tires shown cross-hatched interconnect modules

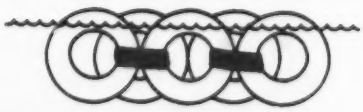

ELEVATION

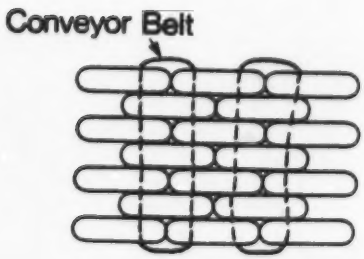

PLAN

FIGURE 3.

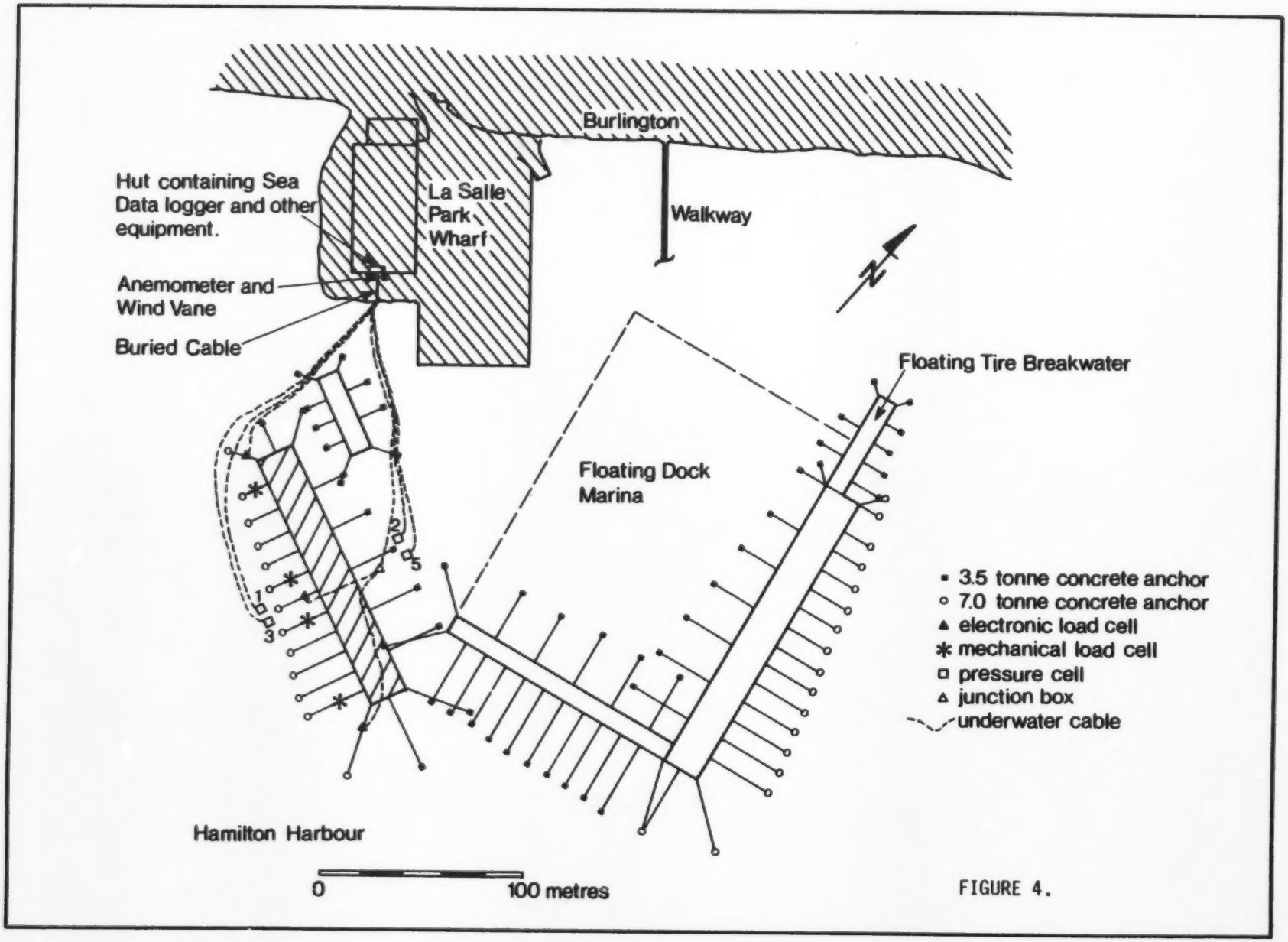
Burlington
Hut containing Sea Data logger and other equipment.
La Salle Park Wharf
Walkway
Anemometer and Wind Vane
Buried Cable
N
Floating Tire Breakwater
Floating Dock Marina
1
2
3
5
3.5 tonne concrete anchor
7.0 tonne concrete anchor
electronic load cell
mechanical load cell
pressure cell
junction box
underwater cable
Hamilton Harbour
0
100 metres

FIGURE 4.

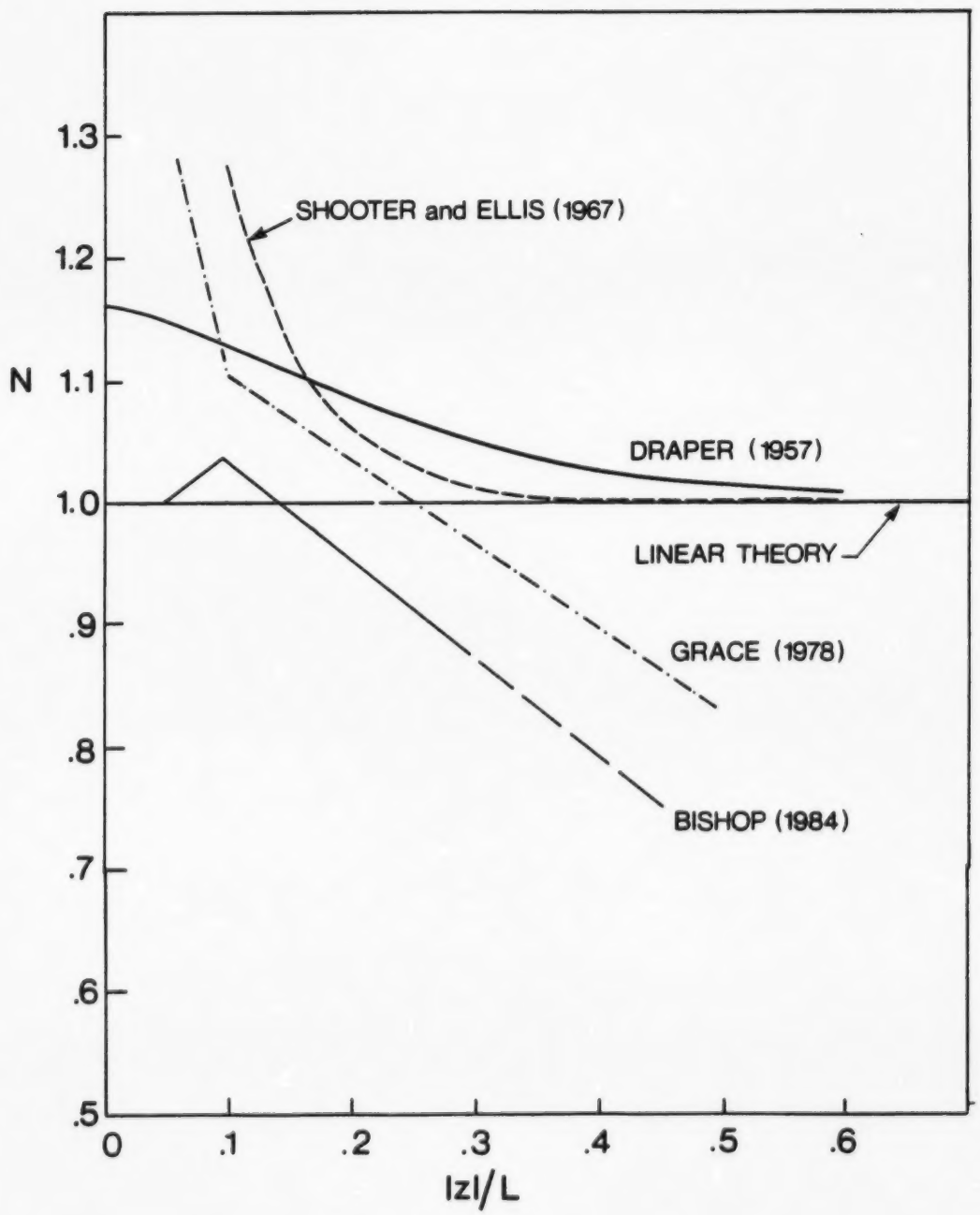
1.3
1.2
N 1.1
1.0
.9
.8
.7
.6
.5
0
.1
.2
.3
.4
.5
.6
|z|/L
SHOOTER and ELLIS (1967)
DRAPER (1957)
LINEAR THEORY
GRACE (1978)
BISHOP (1984)

FIGURE 5.

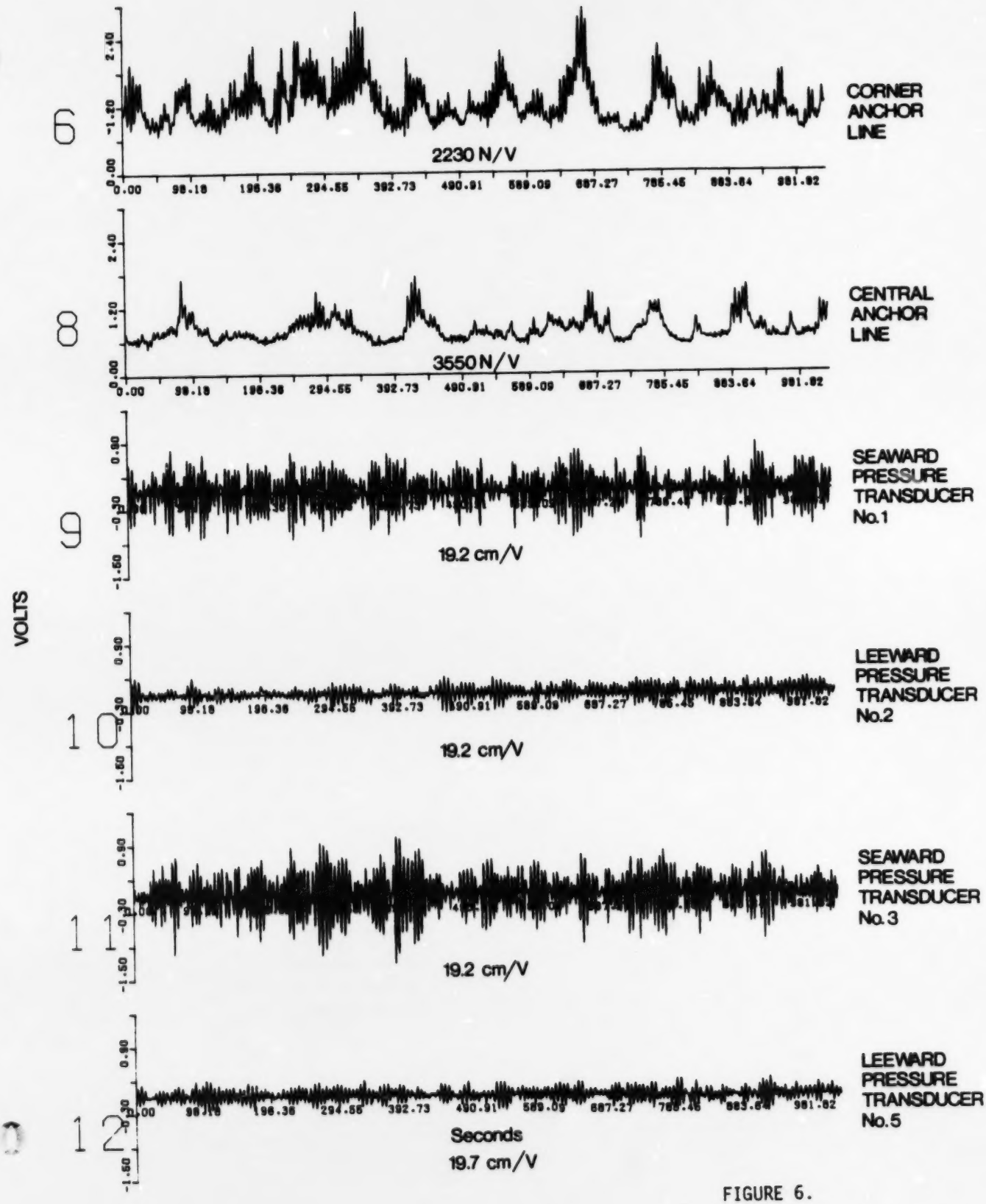
VOLTS
6
2230 N/V
CORNER ANCHOR LINE
8
3550 N/V
CENTRAL ANCHOR LINE
9
19.2 cm/V
SEAWARD PRESSURE TRANSDUCER No.1
10
19.2 cm/V
LEEWARD PRESSURE TRANSDUCER No.2
11
19.2 cm/V
SEAWARD PRESSURE TRANSDUCER No.3
12
Seconds
19.7 cm/V
LEEWARD PRESSURE TRANSDUCER No.5

FIGURE 6.

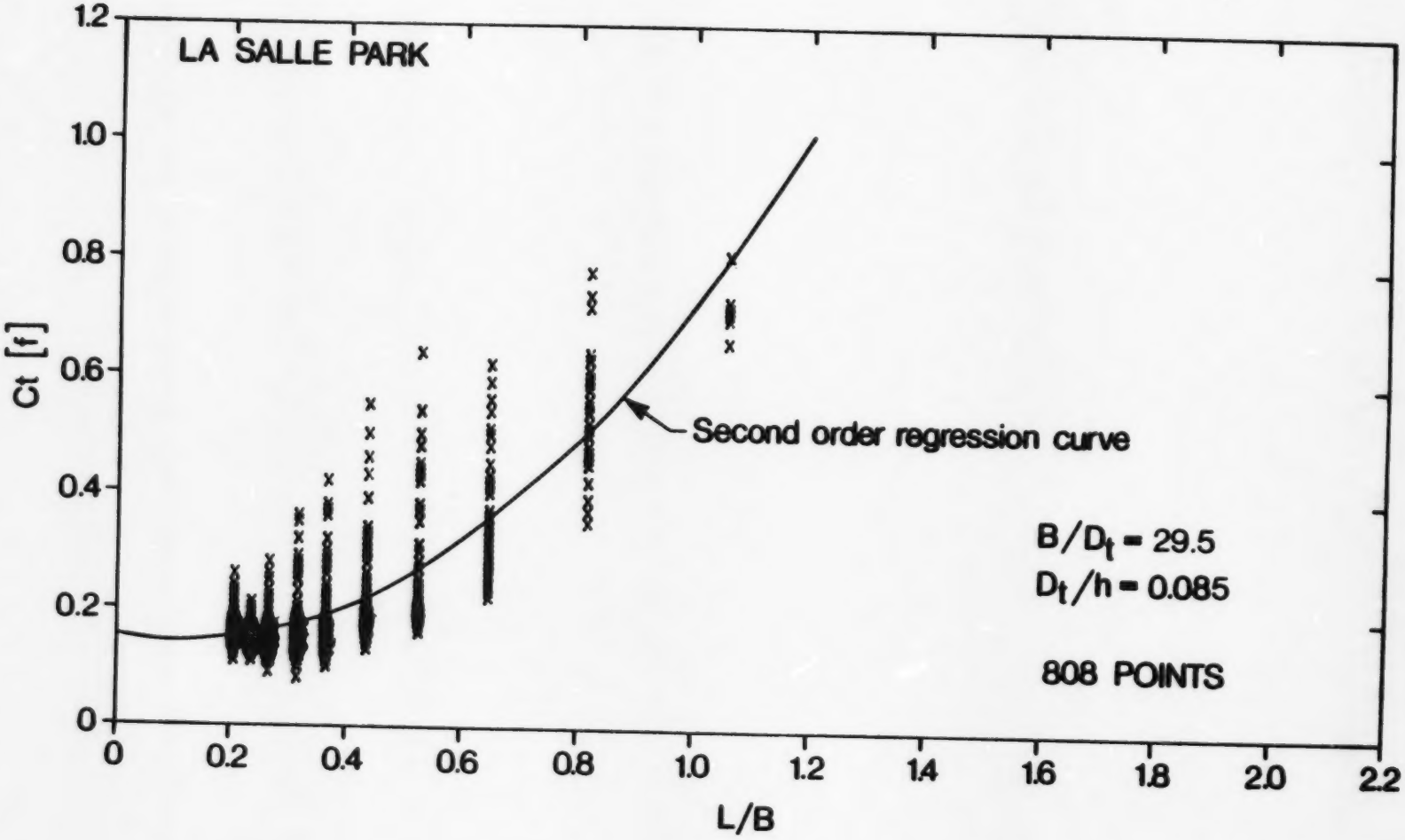
LA SALLE PARK
Ct [f]
L/B
Second order regression curve
B/Dt = 29.5
Dt/h = 0.085
808 POINTS
0
0.2
0.4
0.6
0.8
1.0
1.2
1.4
1.6
1.8
2.0
2.2

FIGURE 7.

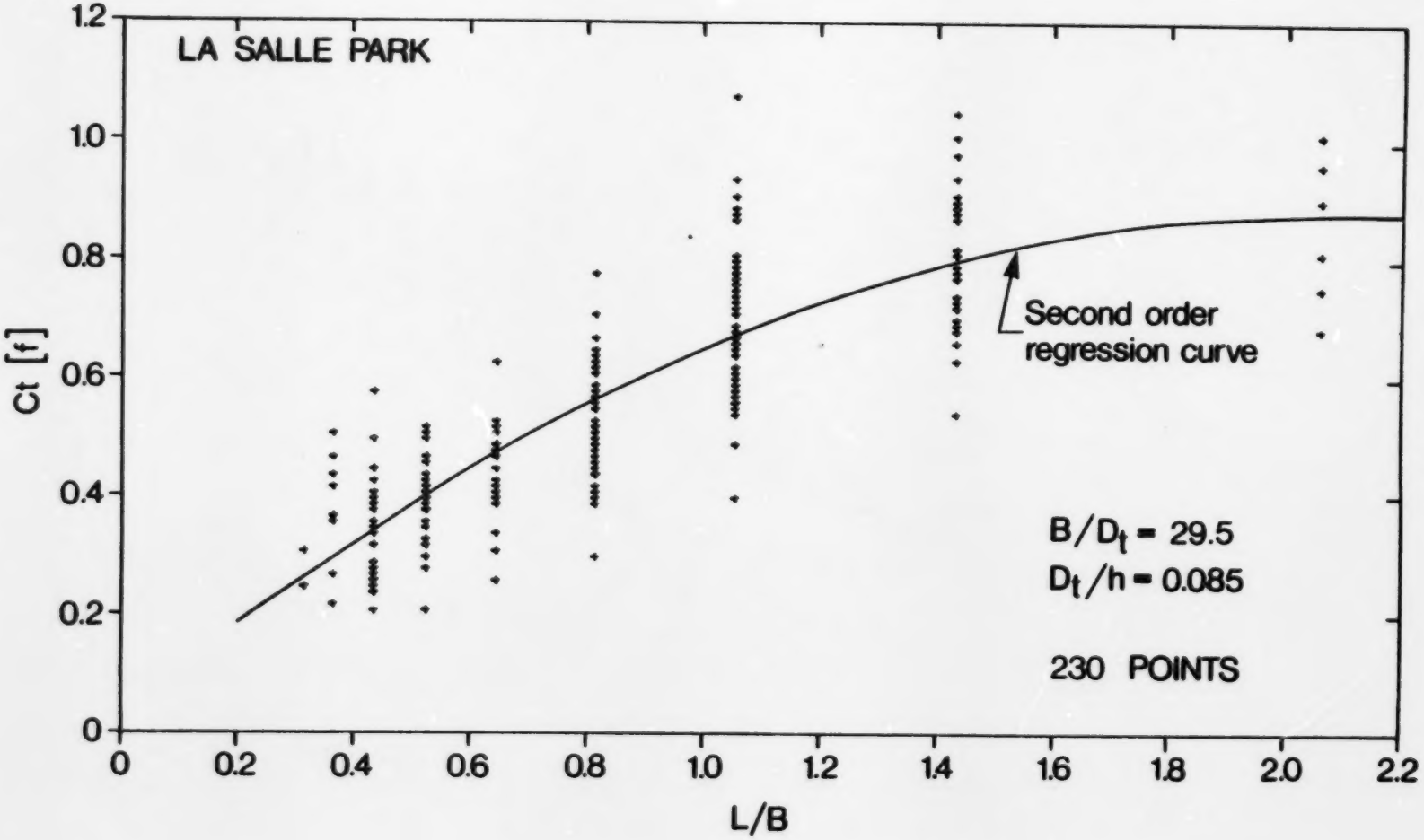
LA SALLE PARK
Second order
regression curve
B/Dt = 29.5
Dt/h = 0.085
230 POINTS
Ct [f]
L/B
0
0.2
0.4
0.6
0.8
1.0
1.2
1.4
1.6
1.8
2.0
2.2

FIGURE 8.

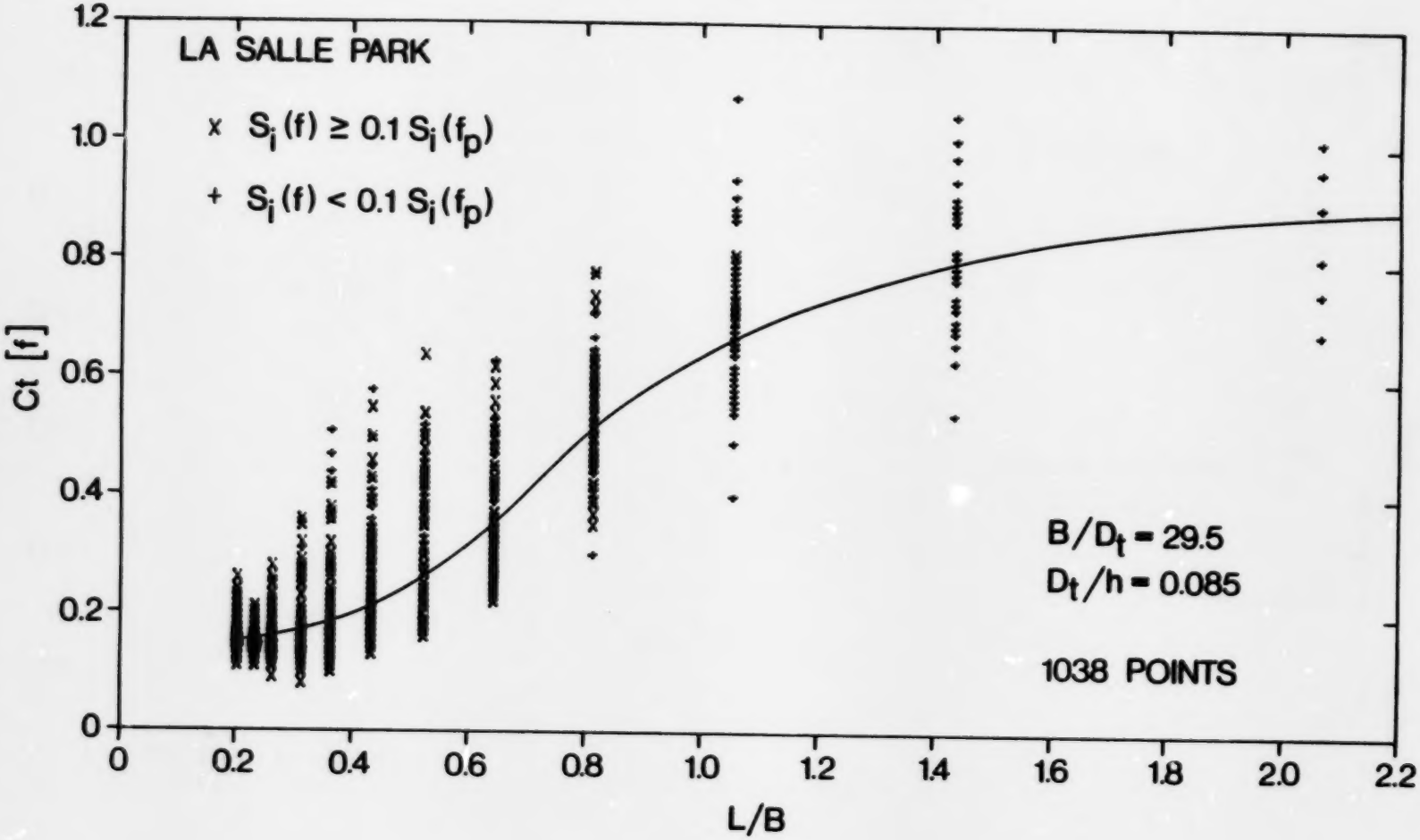
LA SALLE PARK
x $S_i(f) \geq 0.1\, S_i(f_p)$
+ $S_i(f) < 0.1\, S_i(f_p)$
$B/D_t = 29.5$
$D_t/h = 0.085$
1038 POINTS
Ct [f]
L/B
0
0.2
0.4
0.6
0.8
1.0
1.2
1.4
1.6
1.8
2.0
2.2

FIGURE 9.

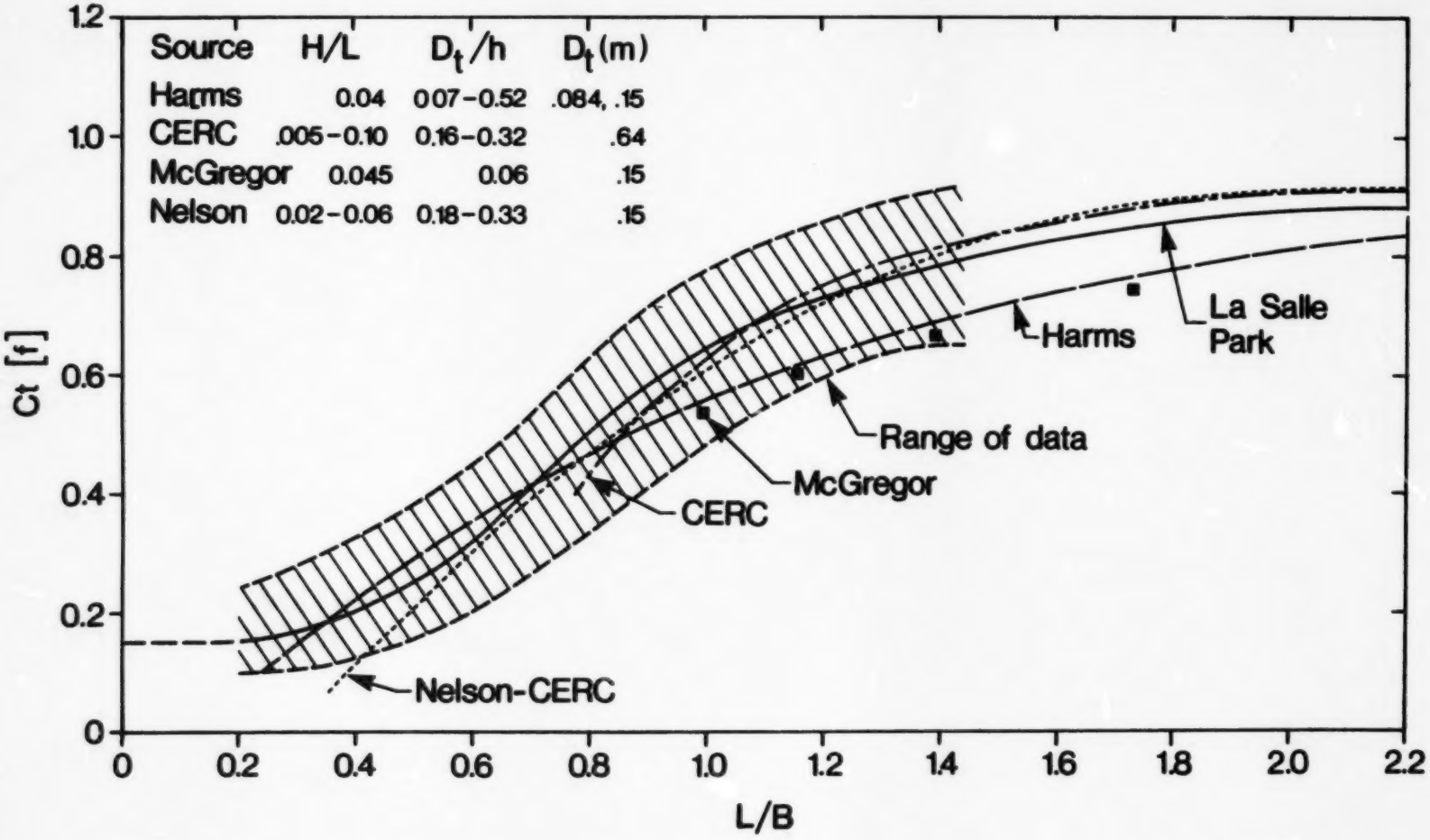
Source H/L D_t/h D_t(m)
Harms 0.04 007-0.52 .084, .15
CERC .005-0.10 0.16-0.32 .64
McGregor 0.045 0.06 .15
Nelson 0.02-0.06 0.18-0.33 .15
Ct [f]
L/B
Harms
La Salle Park
Range of data
McGregor
CERC
Nelson-CERC
0
0.2
0.4
0.6
0.8
1.0
1.2
1.4
1.6
1.8
2.0
2.2

FIGURE 10.

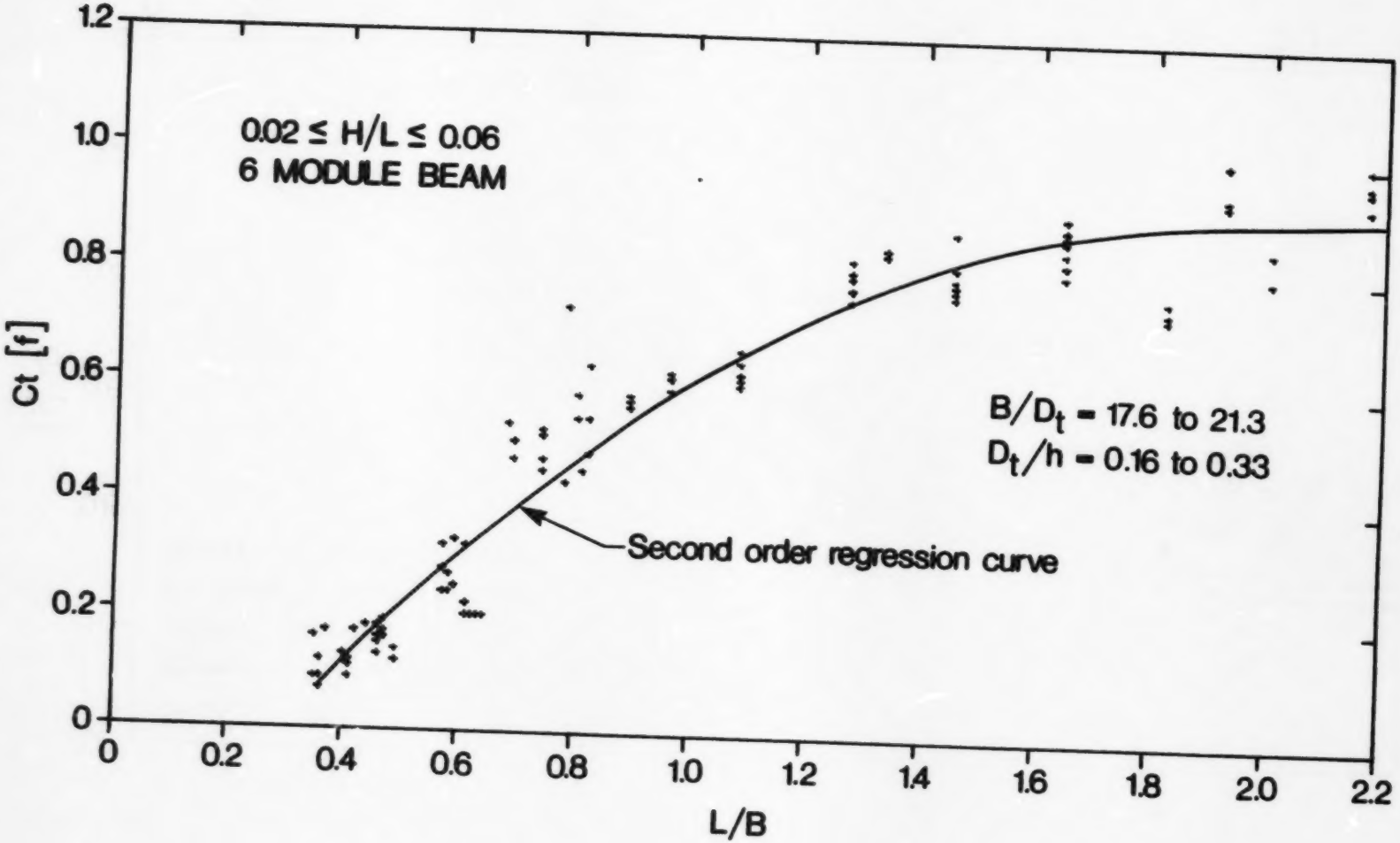
0.02 ≤ H/L ≤ 0.06
6 MODULE BEAM
B/Dt = 17.6 to 21.3
Dt/h = 0.16 to 0.33
Second order regression curve
Ct [f]
L/B
0
0.2
0.4
0.6
0.8
1.0
1.2
1.4
1.6
1.8
2.0
2.2

FIGURE 11.

LASALLE PARK MARINA FLOATING TIRE BREAKWATER
WATER SURFACE ELEVATION VARIANCE POWER SPECTRA

Date: 1982/11/12 Time: 1117 Max. Ordinate = 2055 cm^2/Hz

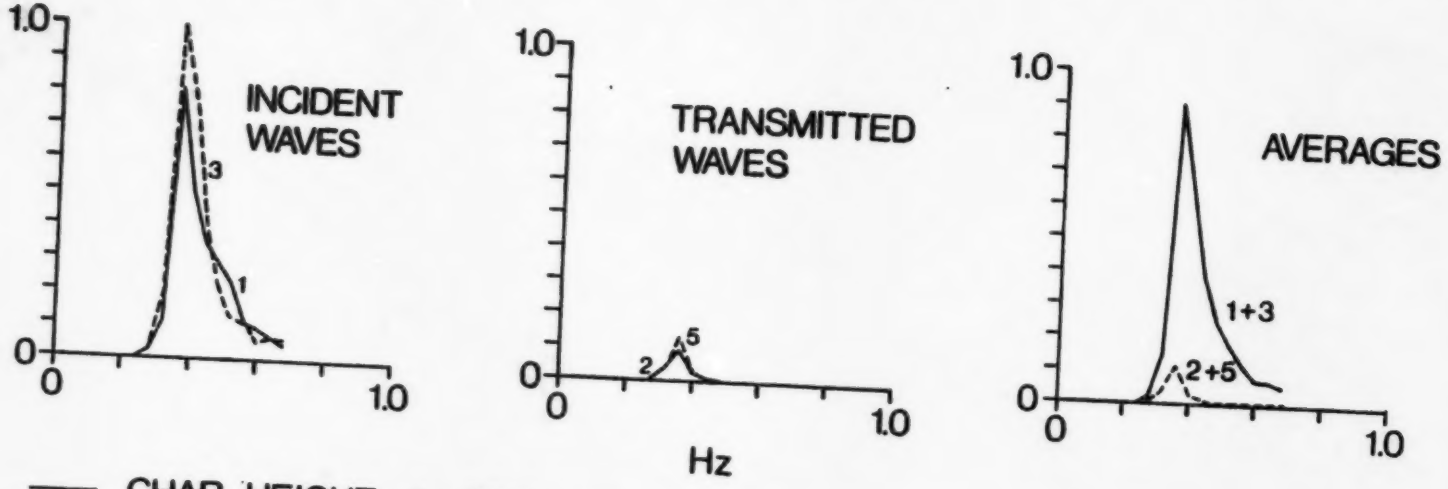

—— CHAR. HEIGHT 1 = 63.8 cm 2 = 17.5 cm 1+3 = 65.4 cm
----- CHAR. HEIGHT 3 = 67.0 cm 5 = 19.1 cm 2+5 = 18.3 cm
—— PEAK FREQ. 1 = .36 Hz 2 = .36 Hz 1+3 = .36 Hz
----- PEAK FREQ. 3 = .36 Hz 5 = .36 Hz 2+5 = .36 Hz

FIGURE 12.

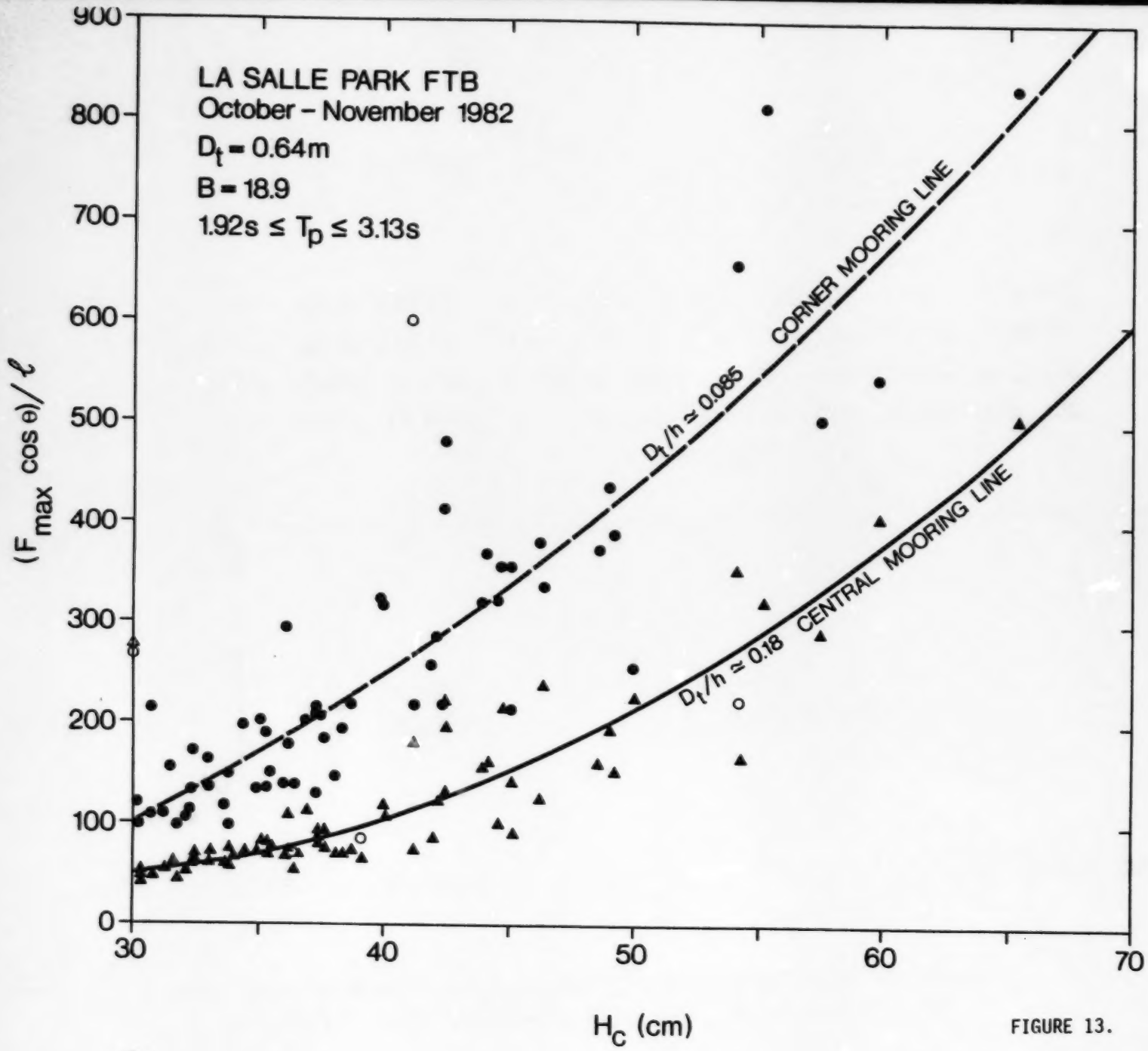
LA SALLE PARK FTB
October – November 1982
D_t = 0.64m
B = 18.9
1.92s ≤ T_p ≤ 3.13s
$D_t/h \simeq 0.085$
CORNER MOORING LINE
$D_t/h \simeq 0.18$
CENTRAL MOORING LINE
$(F_{max} \cos\theta)/\ell$
H_c (cm)
0
100
200
300
400
500
600
700
800
900
30
40
50
60
70

FIGURE 13.

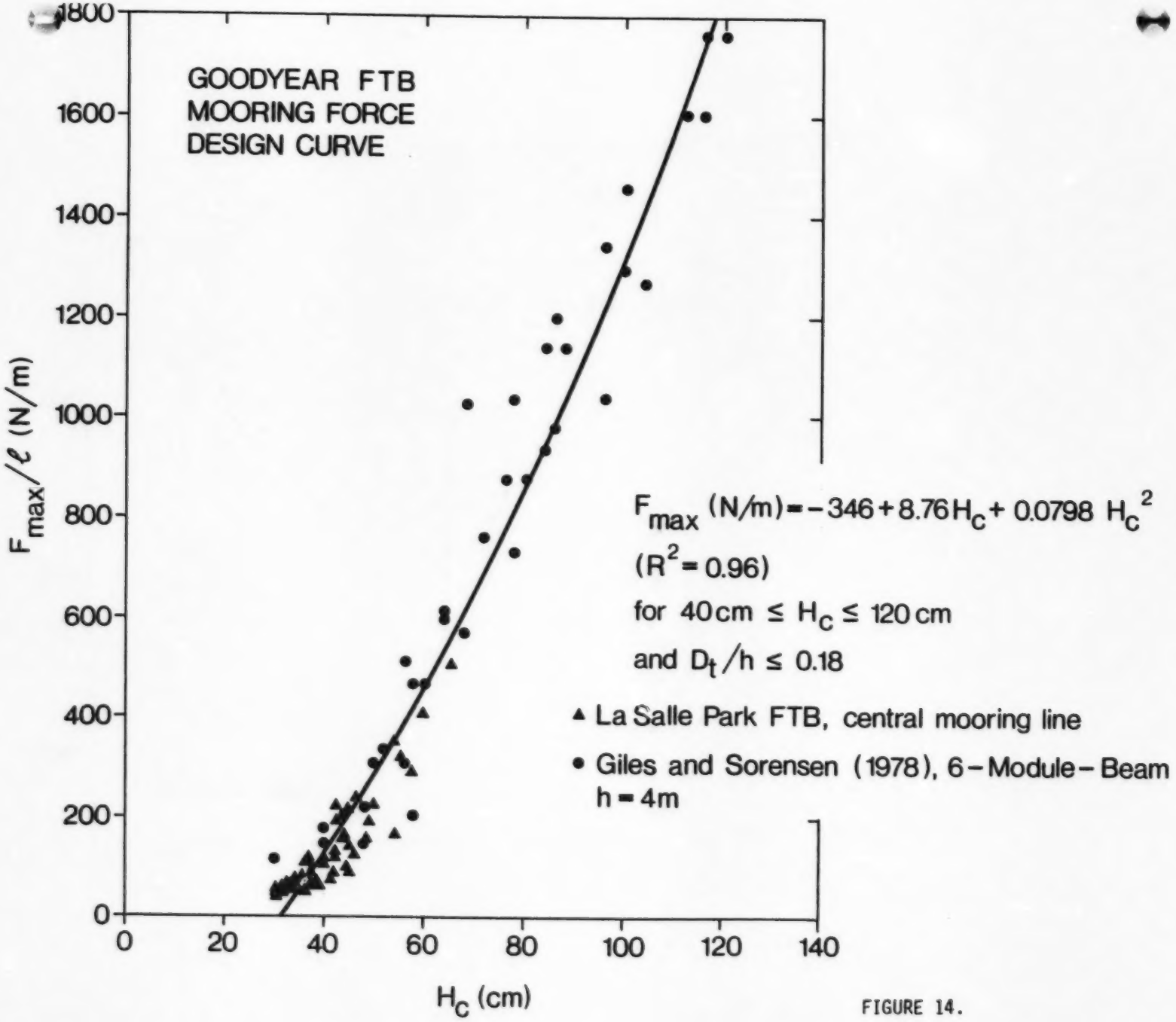
GOODYEAR FTB
MOORING FORCE
DESIGN CURVE
F_{max}/ℓ (N/m)
1800
1600
1400
1200
1000
800
600
400
200
0
0
20
40
60
80
100
120
140
H_c (cm)
F_{max} (N/m) = −346 + 8.76 H_c + 0.0798 H_c^2
(R^2 = 0.96)
for 40 cm ≤ H_c ≤ 120 cm
and $D_t/h \leq 0.18$
▲ La Salle Park FTB, central mooring line
• Giles and Sorensen (1978), 6 − Module − Beam
h = 4m

FIGURE 14.

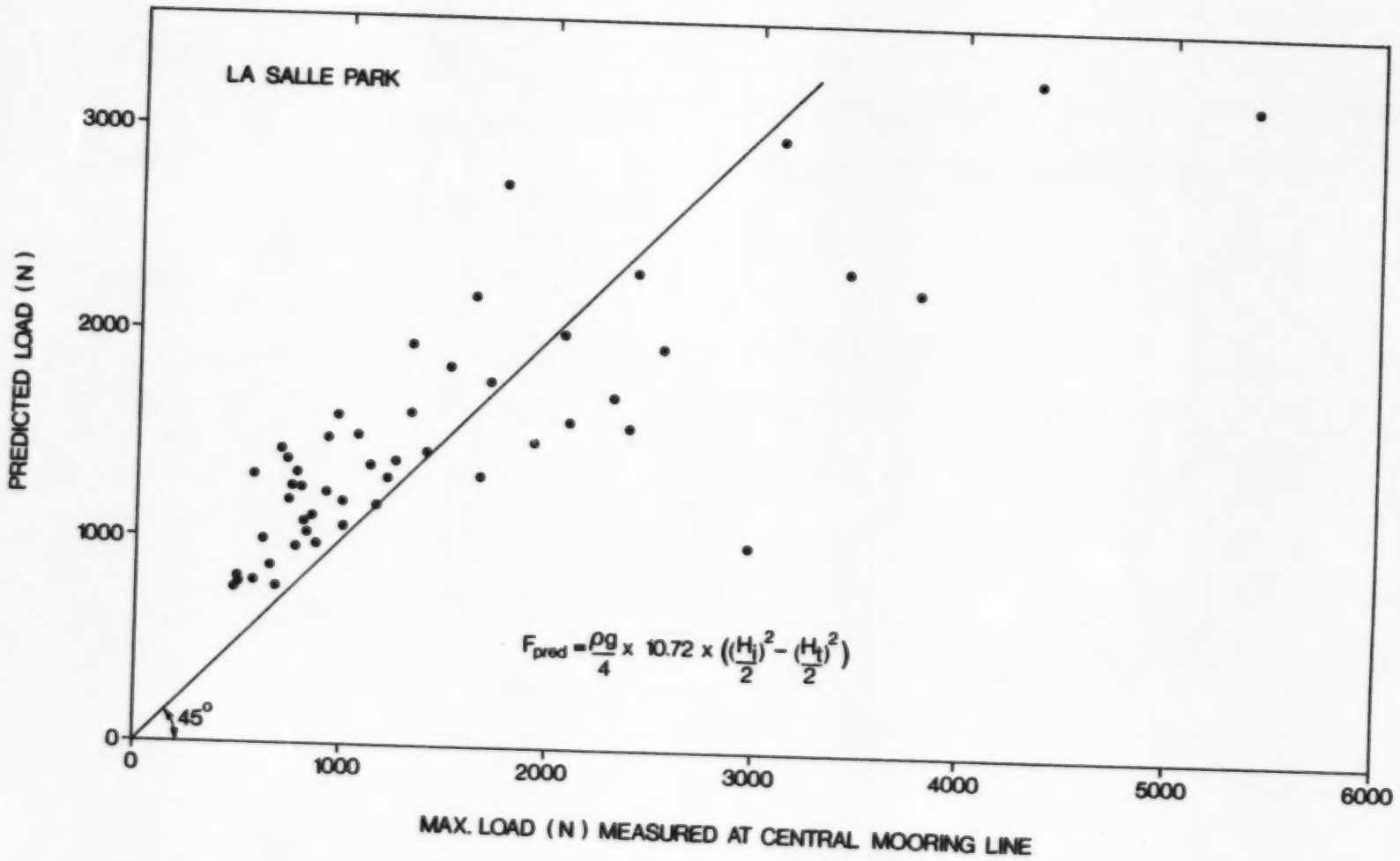
LA SALLE PARK
PREDICTED LOAD (N)
MAX. LOAD (N) MEASURED AT CENTRAL MOORING LINE
$F_{pred} = \frac{\rho g}{4} \times 10.72 \times \left(\left(\frac{H_j}{2}\right)^2 - \left(\frac{H_t}{2}\right)^2\right)$
45°
0
1000
2000
3000
4000
5000
6000

FIGURE 15.